2021

Evolution and development of staminodes in Paronychia (Caryophyllaceae)

Andrea D. Appleton
Georgia Southern University

Evolution and development of staminodes in *Paronychia* (Caryophyllaceae)

An Honors Thesis submitted in partial fulfillment of the requirements for Honors in Biology.

By Andrea D. Appleton

Under the mentorship of John J. Schenk

ABSTRACT

Staminodes are infertile stamens that have evolved numerous times in flowering plants and exhibit a vast array of forms and functions. Variation in staminodes suggests that numerous evolutionary processes underlie their origins, but to understand their how and why they evolved, comparative studies are needed in groups of closely related species. Identifying structures as staminodes is not always straightforward and sometimes requires corroborating phylogenetic and developmental evidence. Staminodial structures in *Paronychia* (Caryophyllaceae), for example, vary in shape and size and have been referred to as both petals and staminodes, rendering their homology uncertain. The development of staminodes was compared across species of *Paronychia*. We tested the hypotheses that structures were either petals or staminodes and by evaluating floral development of fourteen species with scanning electron and light microscopy and conducted ancestral state estimations across phylogenies to infer when staminodes evolved. Staminodes developed between the stamen whorl and carpel, indicating a true staminodial origin. Staminodes evolved prior to the origin of *Paronychia* and were lost at least three times. Staminodes in *Paronychia* began as vestigial stamens following the loss of anthers and were either highly reduced, remained vestigial, or coopted, which we term the vestigial intermediate hypothesis. Our results illustrate a dynamic history of staminodial evolution in *Paronychia* and that selection on the function of staminodes can differ across closely related species.

Thesis Mentor: 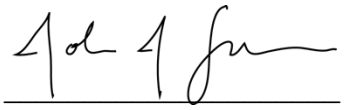
Dr. John J. Schenk

Honors Director: _____
Dr. Steven Engel

April 2021
Department of Biology
University Honors Program
Georgia Southern University

Acknowledgments

This project was funded by the Marie Mellinger Field Botany Research Grant through the Georgia Botanical Society; the Student Research Grant through the Society of Herbarium Curators; the Georgia Southern University Honors Program; the Chandler Scholarship provided by the Chandler family and the Georgia Southern University Department of Biology; and travel awards through the American Society of Plant Taxonomists and the Georgia Southern University Office of Research and Student Government Association. I thank Drs. Andrew Diamanduros, Christopher Cutler, and Vinoth Sittaramane for their assistance with microscopy, Clinton Morse (University of Connecticut) for providing living material of *Pollichia*, the Honors College and the Department of Biology for supporting this work, and Maria von Balthazar, Louis P. Ronse De Craene, and an anonymous reviewer with the International Journal of Plant Sciences for constructive comments that greatly improved an earlier version of this thesis.

Introduction

The evolution of flowers was a key innovation that has led to a remarkable amount of diversity in species and floral forms (Weberling 1989; Chanderbali et al. 2016). Not only does variation exist in the four floral organs (sepals, petals, stamens, and carpels), but an array of non-reproductive novelty has also evolved in flowers, such as nectaries, spurs, and staminodes (Endress 1994; Kramer and Hodges 2010). Among the aforementioned novel floral structures, staminodes —which are infertile stamens— are particularly striking in the sheer amount of innovation and forms that have mostly evolved in response to selection for either alternative functions or stamen reduction (Walker-Larsen and Harder 2000; Ronse De Craene and Smets 2001; Botnaru and Schenk 2019). Staminodes have evolved repeatedly within groups as disparate as monocots, Magnoliids, rosids, and asterids (Walker-Larsen and Harder 2000). Botnaru and Schenk (2019) classified staminodes into three broad categories based on their function and evolutionary history: (1) vestigial staminodes, in which structures are rudimentary and do not produce pollen; (2) fodder staminodes, in which structures produce inviable pollen to encourage palynivore visitation without sacrificing viable pollen, such as in *Commelina* L. (Commelinaceae; Walker-Larsen and Harder 2000); and (3) functionally coopted staminodes, in which structures have evolved a novel function, such as in *Penstemon* Schmidel (Plantaginaceae; Walker-Larsen and Harder 2000). Walker-Larsen and Harder (2000) and Ronse De Craene and Smets (2001) expounded compelling arguments that staminode evolution has been dynamic across angiosperms when examined broadly, but recent work by Pischtschan et al. (2010), Rodríguez-Riaño et al. (2015), and Botnaru and Schenk (2019) have demonstrated that staminode evolution could also be dynamic in

clades of recently evolved, close relatives. Studying the dynamic nature of staminodes among groups that evolved staminodes relatively long ago can be limited because extinction events and additional morphological changes have the potential to obscure patterns of evolution. Studying staminode evolution in a clade of close relatives, conversely, has the potential to illuminate the causes of staminode evolution unconvoluted by other evolutionary processes.

Paronychia Mill. (Caryophyllaceae) is a genus of 110 species, among which the majority, but not all, species are described as containing staminodial structures (Hartman et al. 1997). The genus in the broad sense originated at least 24.87–39.71 mybp, but the New World colonization began diversifying at least 4.50–8.63 mybp (Schenk et al. 2018). Flowers of *Paronychia* are relatively small (< 3 mm in length) and (mostly) bisexual, containing five white, green, yellow, or brown sepals; two to five stamens; five staminodial structures (if present); and two to three carpels (Ronse De Craene 2020). Staminodial structures are filamentous and positioned alternate of the sepals, situated where petals would be anticipated to occur in complete flowers. The homology of staminodial structures, consequently, are not completely clear. In a monograph of *Paronychia*, for example, Chaudhri (1968) described these structures as reduced petals. The nature of petaloid and staminodial structures in Caryophyllaceae has since been challenged (Ronse De Craene and Smets 2001; Brockington et al. 2013; Wei and Ronse De Craene 2019). Greenberg and Donoghue (2011) determined that flowers of Caryophyllaceae were ancestrally apetalous with five stamens based on phylogenetic results, but Wei and Ronse De Craene (2019) concluded that flowers of Caryophyllaceae were ancestrally petalous and had ten stamens based on phylogenetic and developmental

results, but some species have since lost petals and five of the ancestral stamens. Although petals are hypothesized to have evolved from stamens more broadly in Caryophyllaceae (Ronse De Craene 2007), and hence could be referred to as staminodes in their own right (but see Wei and Ronse De Craene 2019), a distinction can be made between petals and staminodes by assessing the homology of the structures. To avoid confusion of terms, we will refer to infertile structures derived from stamens as “staminodes” and, following Wei and Ronse De Craene (2019), “petals” as “petaloids.” We will refer to the structures in alternisepalous positions as "staminodial structures" until their homology is assessed.

The homology of staminodes is often, but not always, straightforward to interpret (Ronse De Craene and Smets 2001), but homology assessment is essential if we are to understand staminode evolution (Hufford 2003). In fodder staminodes, for example, assessing homology is straightforward because they are positioned in an androecial whorl and form what are clearly a filament and anther that produces sterile pollen. In other species, the staminodes arise by splitting of the stamen primordia (Ronse De Craene and Smets 2001), making a clear association of staminodes being derived from the androecial whorl. The homology of staminodes, however, can also be less obvious. In some flowers, staminodes have been structurally and positionally modified to the degree that their homology is difficult to assess (Ronse De Craene and Smets 2001). Flowers in several genera of the Hamamelidaceae, for example, have multiple sets of sterile floral organs (phyllomes, nectaries, and staminodes) which are difficult to distinguish from one another and are not likely derived from the same structures (Mione and Bogle 1990; Ronse De Craene and Smets 2001). Homology of staminodes in other groups, such as

Paronychia, are obscured because the fully developed staminodes appear to be positioned alternate of the sepals, where petaloids are expected to develop.

Homology can be assessed with three criteria: phylogenetic homology, structural homology, and positional homology (Hufford 2003). Phylogenetic homology refers to similarity due to a single evolutionary origin, where the structures in all of its forms are inherited from a common ancestor (Albert et al. 1998; Ronse De Craene and Smets 2001; Hufford 2003). Structural homology is inferred through similarity of forms and their development (Albert et al. 1998; Hufford 2003), but is agnostic to the evolutionary history of the structures. Finally, positional homology is assessed through similarity of the position of structures and where they develop (Albert et al. 1998). Among the three homology criteria, assessing the phylogenetic homology of structures is key to making informed comparisons (Ochoterena et al. 2019). Phylogenetic homology is best assessed by estimating character state transitions across an independent phylogeny (Hufford 2003). Comparative and evolutionary-developmental (Evo-Devo) approaches are essential to assess structural and positional homology of organs at multiple stages of development (Ronse De Craene and Smets 2001). Evo-Devo studies can uncover the relationship between individual development and evolutionary morphological plasticity both at molecular and organismal levels (Müller 2007), allowing us to visualize how and when floral organs develop and infer their evolutionary origins.

We studied the evolution of staminodes among close relatives in a North American clade of *Paronychia*. We hypothesized that staminodial structures in *Paronychia* are staminodes as opposed to petaloids by applying a comparative Evo-Devo approach to assess the phylogenetic, structural, and positional homology of the structures.

To test the above hypothesis and to determine the modes of staminode evolution, we analyzed phylogenetic data with developmental series taken from scanning electron and light microscopy.

Materials and Methods

Sampling

Fourteen species of *Paronychia* were sampled for developmental analyses (Appendix 1). Only staminate flowers of the dioecious and sexually dimorphic *P. chartacea* Fernald ssp. *chartacea* (Anderson 1991) were included in this study, as the female flowers rarely have staminodes (personal observation) and sampling male flowers allowed for important comparisons of staminodes to stamens. Outgroup taxa included *Pollichia campestris* Ait. and *Stipulicida setacea* Michx. (Appendix 1). Both *Pollichia* and *Stipulicida* were traditionally recognized as part of the same subfamily as *Paronychia*, the Paronychioidea, but recent work suggested *Pollichia* is more closely related to *Paronychia*, being placed in the tribe Paronychieae. The former taxa are both more distantly related to *Stipulicida*, which is placed in the tribe Polycarpeae (Harbaugh et al. 2010). Multiple individuals were haphazardly sampled from natural populations by maximizing the distance between collected individuals. Herbarium vouchers were collected and deposited in the Georgia Southern University Herbarium (GAS), and plant tissues were immediately fixed in Formaldehyde-Acetic acid-Alcohol (FAA), or 70% vodka for samples collected in Texas, U.S.A. Samples remained in FAA or vodka for at least one week and were then transferred to 70% ethanol and stored.

Light Microscopy

Samples were prepared for light microscopy with modifications made to methods outlined in Ruzin (1999, pages 57–119). Flowers were removed and transferred through a stepwise ethanol dehydration series (70%, 80%, 90%, 95%, 100%, and 100% for 60 minutes each) and then transferred to a 1:1 solution of 100% EtOH and Tertiary Butyl Alcohol (TBA) for 24 hours. Samples were transferred to a solution of 25:75 EtOH:TBA and 0.1% Safranin O and incubated at 58°C for one hour. Samples were then transferred through a 25:75 solution of EtOH:TBA, 100% TBA, and 100% TBA, each for one hour and incubated at 58°C. Samples were then transferred to 85 x 85 x 24 mm weighing boats and covered with 100% TBA. Paraplast Plus (Leica Biosystems St. Louis, LLC, Buffalo Grove, Illinois, USA) tissue embedding medium was added to fill the weighing boats, and samples were incubated at 58°C until all TBA evaporated. Samples were periodically checked to make sure they remained submerged in TBA and/or paraffin. After all TBA was evaporated, samples were cooled to room temperature to solidify and were mounted onto cassettes for sectioning on a Leica RM2235 Rotary Microtome at 10 μm. Ribbons were expanded on an adhesive-coated slide by floating them on dH_2O warmed to 42°C. Slides were kept at 42°C for at least 24 hours to allow the sections to adhere to the slide as the dH_2O evaporated.

Mounted slides were transferred through a xylene-ethanol series to remove paraffin, by transferring the slides at five minutes each through 100% xylene, 100% xylene, 1:1 xylene:EtOH, 100% EtOH, 100% EtOH, 95% EtOH, and 70% EtOH. Slides were then transferred to a Safranin O staining solution (Ruzin 1999) for one to two hours. Excess stain was rinsed in dH_2O using a wash bottle, and slides were transferred to a

solution of 95% EtOH with the addition of 0.5% picric acid for ten seconds to differentiate the stain. The picric acid reaction was halted by transferring the slides to a solution of 100 mL 95% EtOH with an additional four drops of ammonium hydroxide, then moved to 100% EtOH for ten seconds and counterstained with Fast Green staining solution (Ruzin 1999) for 15 seconds. Excess stain was rinsed with a used clearing solution and then a second clearing solution for ten seconds each. Slides were then moved to a solution of xylene and two drops of 100% EtOH for ten seconds, rinsed with xylene for ten seconds, and transferred to xylene to soak until a coverslip was applied with Permount (Electron Microscopy Sciences, Hartfield, Pennsylvania, USA) mounting medium. Mounted slides were left to dry on a slide warmer at 42°C for at least 24 hours and imaged with Eclipse LV100ND compound scope with Nikon Digital Sight DS-Fi2 (Nikon Corporation, Tokyo, Japan).

Scanning Electron Microscopy

Flowers were removed and transferred through a stepwise ethanol dehydration series as above. Specimens were critical-point dried with a LADD Research Industries Critical Point Dryer (Model 28000) using liquid carbon dioxide as the transitional fluid according to the manufacture's protocol. Dried material was mounted onto carbon-tabbed stubs and further dissected as needed. Stubs were sputter coated using a Denton Vacuum Desk II Sputter Coater with a gold or gold-palladium target for 60 seconds at 35 milliamps. Flowers were examined and imaged with a JEOL JSM-6610LV Scanning Electron Microscope. Images were edited only to optimize contrast and remove backgrounds in Photoshop (Adobe Inc., San Jose, California).

Ancestral Character Estimations

Ancestral character estimations were conducted on chronograms from Schenk et al. (2018) using the Ape (Paradis et al. 2004) and Phytools (Revell 2012) packages in the statistical program R (R Development Core Team 2005) to determine the evolutionary transitions of staminodes in *Paronychia*. Staminode presence or absence were included in the analysis based on personal observation, Flora of North America (Hartman et al. 2005), and a monograph of Paronychiinae (Appendix S1; Chaudhri 1968). Four transition models were fit onto the data. The first model, the equal rates model, parameterized a single transition rate for both transitions to and from staminodes (Harmon et al. 2008). The second model, the all rates different model, allowed for a different transition rate from staminode to stamen than from stamen to staminode (Harmon et al. 2008). The last two models were special cases of the all rates different model in which one rate was set equal to zero. By setting one of the two rates to zero, the two irreversible models allowed only for a transition from no staminodes to staminodes, or the reverse, respectively. Model fit was assessed with AIC values (Akaike 1974), where we preferred the more complex model only if it was greater than two AIC values compared to models with fewer parameters. The models were evaluated and ancestral characters were inferred with maximum likelihood (Felsenstein 1981) in the APE package, the latter of which was also estimated with the Bayesian approach of stochastic character mapping (Huelsenbeck et al. 2003) in the Phytools package. Stochastic character mapping was conducted with 1000 simulated histories across the 95% HPD chronogram estimated from Schenk et al. (2018). Stochastic character mapping analyses were repeated across 500 trees randomly

sampled from the post-burn-in portion of the posterior distribution of trees from Schenk et al. (2018). Analyses were conducted with 10 simulated histories on each phylogeny for a total of 5000 analyses.

Results

Floral descriptions

Paronychia–Flowers were usually pentamerous with five sepals, five antesepalous stamens, and five alternisepalous staminodes when present (Figs. 1–2, S1–S4). The merosity of *P. canadensis* Wood and *P. fastigiata* (Raf.) Fernald were two exceptions, with flowers that contained 2–3 stamens (Figs. 2, S5), as well as *P. chartacea* ssp. *chartacea*, in which flowers usually contained four stamens (Fig. 2). Flowers developed centripetally after the prophylls initiated, starting with the calyx. The first anther to develop (termed anther 1) arose opposite of the first sepal to develop (sepal 1), followed by the remaining four anthers corresponding to the other four sepals and gynoecium. Stamen filaments developed only after the anther formed and elongation initiated simultaneously with staminodial structures (Figs. 1–2, S2–S4), which were positioned as part of the androecial whorl or just inward from the stamens (Figs. 3, S1). In Figure 1B, for example, anthers have initiated, but in Figure 1C when anthers are more developed, filaments and staminodes concurrently initiate. Staminodial structures were present in all species in at least some flowers or developmental stage, and they varied in length and shape across species. In *P. erecta* (Chapm.) Shinners, *P. rugelii* Shuttlew. ex Chapm., *P. americana* Fenzl ex Walp., *P. drummondii* Torr. & A. Gray, *P. baldwinii* (Torr & A. Gray) Fenzl, *P. lindheimeri* Engelm. ex A. Gray, *P. jamesii* Torr. & A. Gray,

and *P. sessiliflora* Nutt., staminodial structures developed at similar times and were subulate to filiform, being similar in size and shape to mature filaments in fertile stamens of the same flower (Figs. 1, S2–S4). In *P. patula* Shinners and *P. herniarioides* Michx., staminodial structures developed at similar times but were broader and more subulate at maturity compared to filaments of the same flower (Figs. 1, S2, S3, S4). Staminodial structures in flowers of *P. argyrocoma* (Michx.) Nutt. initiated, but soon terminated development, and often, only three or four staminodial structures formed (Fig. S3). Staminodial structures and filaments in staminate flowers of *P. chartacea* ssp. *chartacea* also initiated but quickly terminated development, resulting in shorter stamens compared to *P. argyrocoma*. Often, only four stamens developed in *P. chartacea* ssp. *chartacea*, and occasionally, only one to four staminodial structures formed (Figs. 2, S2, S4). Only some flowers of *P. canadensis* and *P. fastigiata* produced staminodial structures, and when present, they were highly reduced compared to the filaments of the stamens (Figs. 2, S3, S4). In contrast to flowers of other species, staminodial structures in *P. canadensis* and *P. fastigiata* did not initiate at the same time as stamen filaments, but rather were delayed to various later stages of overall floral development after the filaments elongated, but before elongation was complete (Figs. 2, S3, S4).

Pollichia–Flowers are composed of five sepals and five staminodial structures that developed centripetally (Fig. 4). Staminodial structures were broad compared to filaments, dorsiventrally flattened, laterally lobed with an obtuse apex, and were born on an androecial ring (Fig. 4). Stamen numbers varied from 0–2 (Fig. 4) and developed opposite of sepals 4 and 5. Due to a limited amount of material, we were neither able to determine whether staminodial structures or stamens developed first nor whether stamens

were positionally born on the androecial ring because it was unclear if the imaged samples were pistillate or hermaphroditic with uninitiated stamens. The androecial ring developed after staminode initiation.

Stipulicida–Flowers were mostly pentamerous with five sepals, five petaloids, two to three stamens, and no staminodes (Fig. 5). Stamens developed opposite the sepals, and petaloids formed alternate of the sepals and abaxially to the stamens (Fig. 5). Anthers developed rapidly after their initiation, while petaloids elongated and expanded more slowly until the stamen were fully formed, in which case the petaloids rapidly expanded just prior to anthesis (Fig. 5).

Ancestral Character Estimations

The model-fitting approach identified the all rates different model as the best-fit model for the data (Table 1). The next best-fitting model was the equal rates model, which differed by 2.399 AIC units, followed by the loss only model that differed by 3.240 AIC units. The gain only model was the worst-fit model, differing from the all rates different model by 7.588 AIC units (Table 1). Given that the all rates different model fit the data best, we applied it in all subsequent ancestral state analyses. Maximum likelihood analyses based on the top two best-fitting models both inferred three independent losses of staminodes in *Paronychia* (Fig. S6). Maximum likelihood analyses with the all rates different model inferred equivocal states at the root node (Fig. S6A), but a higher likelihood of staminodes present at the root was inferred with the equal rates model (Fig. S6B). Stochastic character mapping inferred staminodes being present as the highest proportion at the root, followed by three losses of staminodes (Fig. 6).

Discussion

Studying the morphological evolution of staminodes in recently evolved, closely related groups such as *Paronychia* has the advantage of revealing complex patterns before they are obscured by subsequent evolutionary transformations through time. We identified staminode evolution in *Paronychia* to be markedly more dynamic than previously understood. Staminodial structures in *Paronychia* have been hypothesized to be staminodes or petaloids (Chaudhri 1968; Ronse De Craene and Smets 2001). Our results support those of Ronse De Craene and Smets (2001) and Wei and Ronse De Craene (2019) by providing evidence that staminodial structures in *Paronychia* are staminodes based on their structural and positional homology, development, and morphological similarity to stamen filaments.

Evidence was not identified supporting the hypothesis that staminodial structures in *Paronychia* are homologous with petaloids. When examining the location of the staminodial structure initiation during development, they are not positionally consistent with where we would expect to locate the corolla: the structures develop nearly alongside the stamens or between the stamens and gynoecium (Figs. 3, S1), as opposed to between the stamens and sepals as would be expected if they were homologous to petaloids. SEM micrographs also do not show that the structures arise by splitting of the stamen primordia, as has been found in the petaloids of other Caryophyllaceae genera (Ronse De Craene 2018), but rather they arise independently after the formation of the anthers (Figs. 1–2, S2–S4).

Images from both SEM and light microscopy suggest that the alternisepalous structures are staminodes. The structures originate at or inside of the antesepalous whorl of stamens (Figs. 3, S1) at approximately the same time filaments initiate (Figs. 1–2, S1–S4). The staminodes retain the developmental timing of the filaments, and both structures elongate and simultaneously complete their development. In mature flowers of most staminodial species, staminodes are morphologically similar to filaments in size and shape and never exceed filaments in length (Figs. 1, 2, S2–S4 column 6). Given the location of where staminodes develop, their form, and their developmental timing, we conclude that the staminodes are homologous to filaments in which anthers fail to initiate. In species in which staminodes are lost (e.g., *P. fastigiata*), further reduction is achieved through heterochronic termination of development shortly following initiation.

Flowers of Caryophyllaceae are hypothesized to be ancestrally petalous with ten stamens, but some species have since become apetalous and contain five stamens (Wei and Ronse De Craene 2019). Flowers of *Paronychia*, however, exhibit the latter state. All staminodes in *Paronychia* are apparently homologous with one another and likely evolved prior to its origin (Fig. 6). Staminodes in *Paronychia* have been referred to as vestigial (Ronse De Craene and Smets 2001). Botnaru and Schenk (2019) defined vestigial staminodes as those that have lost their reproductive function and neither produce pollen nor have been coopted for a secondary function. Although we made attempts to determine the staminode function through video recordings to document whether pollinators interact with these structures, observations were inconclusive due to the small size of the flowers and infrequent pollinator visitations. If staminodes in *Paronychia* are vestigial, they would not have a secondary function, but we also

predicted that they would be diminutive to adjacent filaments and have a loss of vascular tissue, a feature common in vestigial organs that is observed in other rudimentary staminodes (Arber 1933). These predictions were largely supported by our results (Figs. 1–3, S2–S4). In most species, staminodes were diminutive compared to adjacent filaments (Figs. 1–2, S2–S4), and in all species observed with light microscopy, a vascular strand was absent (Fig. 3).

Staminodes in *P. americana, P. baldwinii, P. drummondii, P. erecta*, *P. jamesii*, *P. lindheimeri*, *P. rugelii,* and *P. sessiliflora* were the same size or very slightly reduced compared to adjacent filaments (Figs. 1, S2–S4), supporting the interpretation of them being vestigial. Although determining the evolutionary forces that selected for the loss of reproductive function is beyond the scope of this study, the staminodes in the species above might be in evolutionary stasis, in which selection is not acting positively or negatively on them following the initial selection for reduction of floral size. The above species, alternatively, might also be experiencing stabilizing selection, where the staminodes are performing a function that we have yet to determine. Differentiating between the two hypotheses above is central to understanding the evolution and persistence of staminodes in *Paronychia*.

In species reported to lack staminodes (*P. canadensis*, *P. chartacea* ssp. *chartacea*, and *P. fastigiata*) and in *P. argyrocoma*, staminodes begin to develop concomitantly with filaments but are terminated shortly after they initiate, resulting in rudimentary structures compared to adjacent filaments (Figs. 2, S2–S4). In mature flowers, those terminated staminodes are difficult or impossible to observe, even with the aid of a hand lens because they are so diminutive. We hypothesize that reduction of

staminodes in those species cooccurs with an overall floral reduction (see below for further discussion). The selective forces that promote further floral reductions are not understood well in *Paronychia*.

In contrast to staminodes that retain the shape of stamen filaments and those which are reduced, staminodes in *P. herniarioides* and *P. patula* appear much wider at the base than adjacent filaments and have putatively undergone morphological evolution, supporting the hypothesis that staminodes in some species of *Paronychia* have been coopted for a currently unknown function. If staminodes are indeed coopted in the above species, we hypothesize that they are performing one of the following three functions. We first hypothesize that staminodes in *Paronychia* function as pollinator nectar guides. Staminodes acting as nectar guides and more broadly as visual displays has been observed in the Zingiberales (Specht et al. 2012) and Linaceae (Walker-Larsen and Harder 2000), but those in *Paronychia* are not conspicuous and not likely to aid in attracting pollinators (Figs. 1–2, S2–S4). Our second hypothesis is that staminodes are coopted to function as pollinator landing platforms. In *Herrania purpurea* (Pittier) R.E. Shult. (Malvaceae), for example, staminodes function as landing platforms during the female phase of the flowers (Young 1984; Walker-Larsen and Harder 2000). Our third hypothesis is that staminodes have been coopted to force pollinators to enter the flower from above, rather than from the side. As such, the staminodes could function to either protect the flower from nectar thieves or facilitate pollination by assuring that pollinators come into contact with both anthers and stigmas.

The complex pattern of vestigial and coopted staminodes in *Paronychia* is consistent with what we term the vestigial intermediate hypothesis, which we define as

the evolution of vestigial staminodes prior to being coopted for a secondary function. Walker-Larsen and Harder (2000) observed this pattern of reduction, loss, and functional cooption in the Lamiales and proposed that stamens that first lost their function could more easily be coopted for alternative functions without further disrupting stabilizing selection of reproductive output in the fertile androecial whorl. In *Paronychia*, we argue that staminodes began as vestigial structures following the loss of the anther and subsequently had three fates: they either remained similar to filaments, were lost, or were coopted for a secondary, but unknown, function. Such a process explains why the staminodes of *P. herniarioides* have undergone morphological evolution compared to its filaments but still lack vascular tissue (Fig. 3). A fourth outcome of the vestigial intermediate hypothesis, which was not observed in our data, is an evolutionary reversal to regain a reproductive function. Staminodial ancestors have given rise to descendent lineages that contain fertile stamen in the same position on the basis of phylogenetic comparative analyses and positional homology (Botnaru and Schenk 2019). At least one species of *Paronychia*, *P. sanchez-vegae* (Montesinos-Tubee et al. 2018), has been observed to contain ten stamens. We were unable to sample specimens of *P. sanchez-vegae* in this study, but the presence of ten stamens could represent a reversal where the five staminodes regained their reproductive function. The vestigial-intermediate pattern is unlikely to be an explanation for staminode evolution across all groups. In *Mentzelia* section *Bartonia* (Loasaceae), for example, Botnaru and Schenk (2019) hypothesized that staminodes coopted for visual display evolved as selection favored broader filaments, and therefore staminodes could evolve directly from stamen without first experiencing a vestigial stage.

Combining developmental and phylogenetic data illuminated the complexities of the evolutionary history of staminodes in *Paronychia*. Each of the three observed staminode morphologies have evolved multiple times independently across the phylogeny (Figs. 6, S4). Filamentous staminodes, which we refer to as vestigial, appear ancestral in our study and have been retained in the majority of descendants (Figs. 6, S4). Vestigial staminodes likely evolved prior to *Paronychia* (Fig. 6). For example, Ronse De Craene and Smets (2001) and Wei and Ronse De Craene (2019) documented *Gymnocarpos decandrus* Forssk. (= *Paronychia decandra* (Forssk.) Rohweder & Urmi-König) as having a similar developmental pathway as what we observe in *Paronychia* in this study, with staminodes resembling vestigial stamen filaments at maturity and do not contain vascular tissues. Species in which staminodes are lost or greatly reduced occur in separate clades, except for *P. canadensis* and *P. fastigiata*, which are sister to one another (Figs. 6, S6). Species with elaborated staminodes, such as *P. herniarioides* and *P. patula*, also occur in distinct clades (Figs. 6, S6). These repeated reductions and elaborations demonstrate a complex history of selection and morphological evolution within a group of close relatives.

An unexpected pattern observed in our developmental results is a correlation of staminode loss with overall floral reduction. Contrary to previous works that suggested *P. canadensis*, *P. chartacea* ssp. *chartacea*, and *P. fastigiata* lack staminodes (Hartman et al. 2005), we determined all species to have staminodes initiate and develop to various extents in at least some flowers (Figs. 2, S2–S4). Whereas the ancestor of *Paronychia* has pentamerous flowers (Greenberg and Donoghue 2011; Wei and Ronse De Craene 2019), three of the species in which we observe a reduction or loss of staminodes also contain

fewer stamens. In *P. chartacea* ssp. *chartacea*, we observe a near-loss of staminodes, and stamens are typically reduced to four (Figs. 2, S2, S4). In *P. canadensis* and *P. fastigiata*, which also have a near-loss of staminodes, stamens are reduced to two to three (Figs. 2, S3, S4). Given their sister relationship, stamen loss likely occurred in their most recent common ancestor (Fig. 6), and we find that stamens that develop in position 4 and 5 (occasionally also 3) are the ones that were lost (Fig. S5). In flowers with reduced stamen numbers, it is interesting to compare the partial loss of stamen whorls to the staminodial whorl.

In *Paronychia*, staminodes are typically present in a whole whorl or lost in a whole whorl; we never observed the reduction or loss of staminodes partially within a whorl. Stamens in the antesepalous whorl, however, can be partially lost. In all cases in which one to four stamens were lost, we do not observe staminodes in their place (Figs. 2, S2–S4). Such a pattern begs the question, why do staminodes remain on whole whorls, but no vestigial structures remain on partial whorls of stamens? Is there an unrealized function for the staminodes we classified as vestigial, or is the developmental program of the staminodial whorl so canalized that the structures are not lost? Given the association of reduced stamens and staminodes and the relatively small flower sizes, we hypothesize that the reduction of androecial structures is a consequence of selection for smaller flowers as stamens endure mechanical pressure from the sepals and gynoecium (Wei and Ronse De Craene 2020). The repeated independent loss of staminodes suggests that at least in some species, staminodes might be lost due to disuse, but when considering the harsh sandhill environments in which *Paronychia* grow (Schenk et al. 2018), we hypothesize that staminodes in *Paronychia* have evolved in large part to selection for a

reduction in overall flower size associated with nutrient poor habitats (Galen 1999; Guerrant 1990).

In contrast to the correlation of reduced stamen number associated with the loss of staminodes and reduced flower size in *Paronychia*, *Pollichia campestris* was observed having 1–2 stamens but all five staminodes (Fig. 4). Unlike what we observed in *Paronychia* with a partial loss of later developing stamens in the fertile androecial whorl (Fig. S5), stamens that developed in positions 1–3 (occasionally 4) were lost in *Pollichia* (Fig. 4), but similarly, there are no rudimentary structures or other evidence indicating where stamens were once positioned. Stamen loss was also observed in *Stipulicida setacea*, which has two to three stamens, though staminodes are not present in this species (Fig. 5). Five petaloids are present in the alternisepalous positions of the relatively large flowers of *Stipulicida* compared to *Paronychia* (Fig. 5). Floral reduction in *Paronychia*, *Pollichia*, and *Stipulicida* has likely evolved independently, as has also been shown in *Gymnocarpos* (Wei and Ronse De Craene 2019).

In conclusion, we propose the vestigial intermediate hypothesis as one mechanism by which staminodes evolve, but how widespread this evolutionary phenomenon is and the factors that are important in this evolutionary pathway requires further investigations. Conducting multifaceted approaches that combines morphological variation, development, and phylogenetic comparative methods among recently evolved, closely related species, such as *Paronychia*, provides valuable insight to the intricacies of evolution that might be unobservable when examining only broad patterns across families. Although our results identified that staminode evolution in *Paronychia* was quite dynamic, additional studies that measure the microevolutionary processes that have

selected for staminodial traits, including the filamentous, coopted, and reduced forms, are needed to better understand the selective forces that promoted staminode evolution throughout *Paronychia*.

Literature Cited

Akaike H 1974 A new look at statistical model identification. IEEE Trans on Automat Contr 19:716–723.

Albert VA, MHG Gustafsson, LD Laurenzio 1998 Ontogenic systematics, molecular developmental genetics, and the angiosperm petal. Pages 349–374 *in* DE Soltis, PS Soltis, JJ Doyle eds. Molecular Systematics of Plants, II: DNA Sequencing. Kluwer Academic Publishers, Boston.

Anderson LC 1991 *Paronychia chartacea* ssp. *minima* (Caryophyllaceae): A new subspecies of a rare Florida endemic. SIDA Contrib Bot 14:435–441.

Arber 1933 Floral anatomy and its morphological interpretation. New Phytol 32:231–242.

Botnaru L, JJ Schenk 2019 Staminode evolution in *Mentzelia* section *Bartonia* (Loasaceae) and its impact on insect visitation rates. Bot J Linn Soc 190:151–164.

Brockington S, P Dos Santos, B Glover, L Ronse De Craene 2013 Androecial evolution in Caryophyllales in light of a paraphyletic Molluginaceae. Am J Bot 100:1757–1778.

Chanderbali AS, BA Berger, DG Howarth, PS Soltis, DE Soltis 2016 Evolving ideas on the origin and evolution of flowers: New perspectives in the genomic era. Genetics 202:1255–1265.

Chaudhri MN 1968 A revision of the Paronychiinae. Mededelingen van het Botanisch Museum en Herbarium van de Rijksuniversiteit te Utrecht 285:3–440.

Endress P 1994 Diversity and Evolutionary Biology of Tropical Flowers. Cambridge University Press, United Kingdom.

Endress PK 2001 Origins of flower morphology. J Exp Zool 291:105–115.

Felsenstein J 1981 Evolutionary trees from DNA sequences: A maximum-likelihood approach. J. Mol Evol 17:368–376.

Galen C 1999 Why do flowers vary? The functional ecology of variation in flower size and form within natural plant populations. BioScience 49:631–640.

Greenberg A, M Donoghue 2011 Molecular systematics and character evolution in Caryophyllaceae. Taxon 60:1637–1652.

Guerrant E 1990 Early Maturity, Small Flowers, and Autogamy: A Developmental Connection? Pages 61–84 *in* JH Bock, YB Linhart, GL Stebbins, CE Turner, eds. The Evolutionary Ecology of Plants. Boca Raton, Florida.

Harbaugh DT, M Nepokroeff, RK Rabeler, J McNeill, EA Zimmer, WL Wagner 2010 A new lineage-based tribal classification of the family Caryophyllaceae. Int J Plant Sci 171:185–198.

Harmon LJ, JT Weir, CD Brock, RE Glor, W Challenger 2008 GEIGER: Investigating evolutionary radiations. Bioinformatics 24:129–131.

Hartman RL, JW Thieret, RK Rabeler 2005 *Paronychia* Nailwort. Pages 30–43 *in* FoNAE Committee ed. Flora of North America North of Mexico. Vol. 5, New York and Oxford.

Huelsenbeck JP, R Nielsen, JP Bollback 2003 Stochastic mapping of morphological characters. Syst Biol 52:131–158.

Hufford L 2003 Homology and developmental transformation: Models for the origins of the staminodes of Loasaceae subfamily Loasoideae. Int J Plant Sci 164:S409–S439.

Kramer EM, SA Hodges 2010 *Aquilegia* as a model system for the evolution and ecology of petals. Philos Trans R Soc Lond B Biol Sci 365:477–490.

Mione T, A Bogle 1990 Comparative ontogeny of the inflorescence and flower of *Hamamelis virginiana* and *Loropetalum chinense* (Hamamelidaceae). Am J Bot 77:77–91.

Montesinos-Tubee D, A Cano, L Garcia-Llatas, Y Ju, A Kool 2018 *Paronychia sanchez-vegae* (Caryophyllaceae), a new woody species of *Paronychia* from North Peru. Phytotaxa 334:41–48.

Müller GB 2007 Evo-Devo: Extending the evolutionary synthesis. Nat. Rev. Genet. 8:943–949.

Ochoterena H, A Vrijdaghs, E Smets, R Claßen-Bockhoff 2019 The search for common origin: Homology revisited. Syst Biol 68:767–780.

Paradis E, J Claude, K Strimmer 2004 APE: Analyses of phylogenetics and evolution in R language. Bioinformatics 20:289–290.

Pischtschan E, AC Ley, R Claßen-Bockhoff 2010 Ontogenetic and phylogenetic diversification of the hooded staminode in Marantaceae. Taxon 59:1111-1125.

R Development Core Team 2005 R: A language and environment for statistical computing. http://cranr-projectorg.

Revell LJ 2012 Phytools: An R package for phylogenetic comparative biology (and other things). Methods Ecol Evol 3:217–223.

Rodríguez-Riaño T, FJ Valtueña, JMR López, ML Navarro-Pérez, JL Pérez-Bote, A Ortega-Olivencia 2015 Evolution of the staminode in a representative sample of

Scrophularia and its role as nectar safeguard in three widespread species. Sci Nat 102:1–13.

Ronse De Craene LP 2007 Are petals sterile stamens or bracts? The origin and evolution of petals in the core eudicots. Ann Bot 100:621–630.

Ronse De Craene LP 2018 Understanding the role of floral development in the evolution of angiosperm flowers: Clarifications from a historical and physico-dynamic perspective. Plant J 131:367–393.

Ronse De Craene LP 2020 Gynoecium structure and development in core Caryophyllales: A matter of proportions. Bot J Linn Soc. XX:1–30.

Ronse De Craene LP, EF Smets 2001 Staminodes: Their morphological and evolutionary significance. Bot Rev 67:351–402.

Ruzin SE 1999 Plant Microtechnique and Microscopy. Oxford University Press, Oxford.

Schenk JJ, S Kontur, H Wilson, M Noble, E Derryberry 2018 Allopatric speciation drives diversification of ecological specialists on sandhills. Int J Plant Sci 179:325–339.

Specht CD, R Yockteng, AM Almeida, BK Kirchoff, WJ Kress 2012 Homoplasy, pollination, and emerging complexity during the evolution of floral development in the tropical gingers (Zingiberales). Bot Rev 78:440–462.

Thiers B 2015 Index Herbariorum: A global directory of public herbaria and associated staff.

Walker-Larsen J, LD Harder 2000 The evolution of staminodes in angiosperms: Patterns of stamen reduction, loss, and functional re-invention. Am J Bot 87:1367–1384.

Walker-Larsen J, LD Harder 2001 Vestigial organs as opportunities for functional innovation: The example of the *Penstemon* staminode. Evolution 55:477–487.

Weberling F 1989 Morphology of Flowers and Inflorescences. Cambridge University Press, Cambridge.

Wei L, L Ronse De Craene 2019 What is the nature of petals in Caryophyllaceae? Developmental evidence clarifies their evolutionary origin. Ann Bot 124:281–295.

Wei L, L Ronse De Craene 2020 Hofmeister's Rule's paradox: Explaining the changeable carpel position in Caryophyllaceae. Int J Plant Sci 181:911–925.

Young AM 1984 Mechanism of pollination by Phoridae (Diptera) in some *Herrania* species (Sterculiaceae) in Costa Rica (Sterculiaceae) in Costa Rica. Mecanismo de polinización por Phoridae (Diptera) en algunas especies de *Herrania* (Sterculiaceae) en Costa Rica. Proc Entomol Soc Wash 86:503–518.

Appendix 1. Collection and voucher information for plant material used for scanning electron and light microscopy. All material was collected in the United States. Herbarium codes are consistent with the Index Herbariorum (Thiers 2015).

Outgroup–***Pollichia campestris*** Aiton, University of Connecticut Greenhouse, *Taylor 668* (CONN) *200100492*; ***Stipulicida setacea*** Michaux, Georgia, Irwin County, *A. Appleton 6 and J. Schenk* (GAS).

Ingroup–***Paronychia americana*** Fenzl ex Walp., Georgia, Ben Hill County, *A. Appleton 9 and J. Schenk* (GAS); ***P. americana*** Fenzl ex Walp., Florida, Highlands, *J. Schenk 2543* (GAS); ***P. argyrocoma*** (Michx.) Nutt., Georgia, Lumpkin County, *A. Appleton 66 and J. Schenk* (GAS); ***P. baldwinii*** (Torr. & A. Gray) Fenzl, Georgia, Bryan County, *A. Appleton 1 and J. Schenk* (GAS); ***P. canadensis*** Wood, Ohio, Athens County, *J. Schenk 2601* (BHO); ***P. chartacea*** Fernald **ssp. *chartacea***, Florida, Polk County, *A. Appleton 58 and J. Schenk* (GAS); ***P. drummondii*** Torr. & A. Gray, Texas, Bastrop, *J. Schenk 2552* (GAS); ***P. erecta*** (Chapm.) Shinners, Florida, Wakulla, *J. Schenk 2535* (GAS); ***P. fastigiata*** (Raf.) Fernald, Ohio, Jefferson County, *J. Schenk 2603* (BHO); ***P. herniarioides*** Michx., Georgia, Bulloch, *J. Schenk 2440* (GAS); ***P. jamesii*** Torr. & A. Gray, Texas, Brewster, *J. Schenk 2558* (GAS); ***P. lindheimeri*** Engelm. ex A. Gray, Texas, Llano, *J. Schenk 2551* (GAS); ***P. patula*** Shinners, Florida, Citrus County, *A. Appleton 60 and J. Schenk* (GAS); ***P. rugelii*** Shuttlew. ex Chapm., Florida, Citrus County, *A. Appleton 59 and J. Schenk* (GAS); ***P. sessiliflora*** Nutt., Texas, Hartley, *J. Schenk 2566* (GAS).

Table 1. Likelihood, AIC, and ΔAIC values from ancestral character reconstruction model fitting in which the equal rates model allowed for transitions to occur at equal rates; the all rates different (ARD) model allows for transitions to be separate parameters; the gain only model allows only for the gain of staminodes; and the loss only model allows only for the loss of staminodes.

Model	Likelihood	AIC	ΔAIC
Equal rates	-13.02621	28.05242	2.399
ARD	-10.82648	25.65296	0
Gain only	-15.62070	33.24140	7.588
Loss only	-13.44666	28.89333	3.240

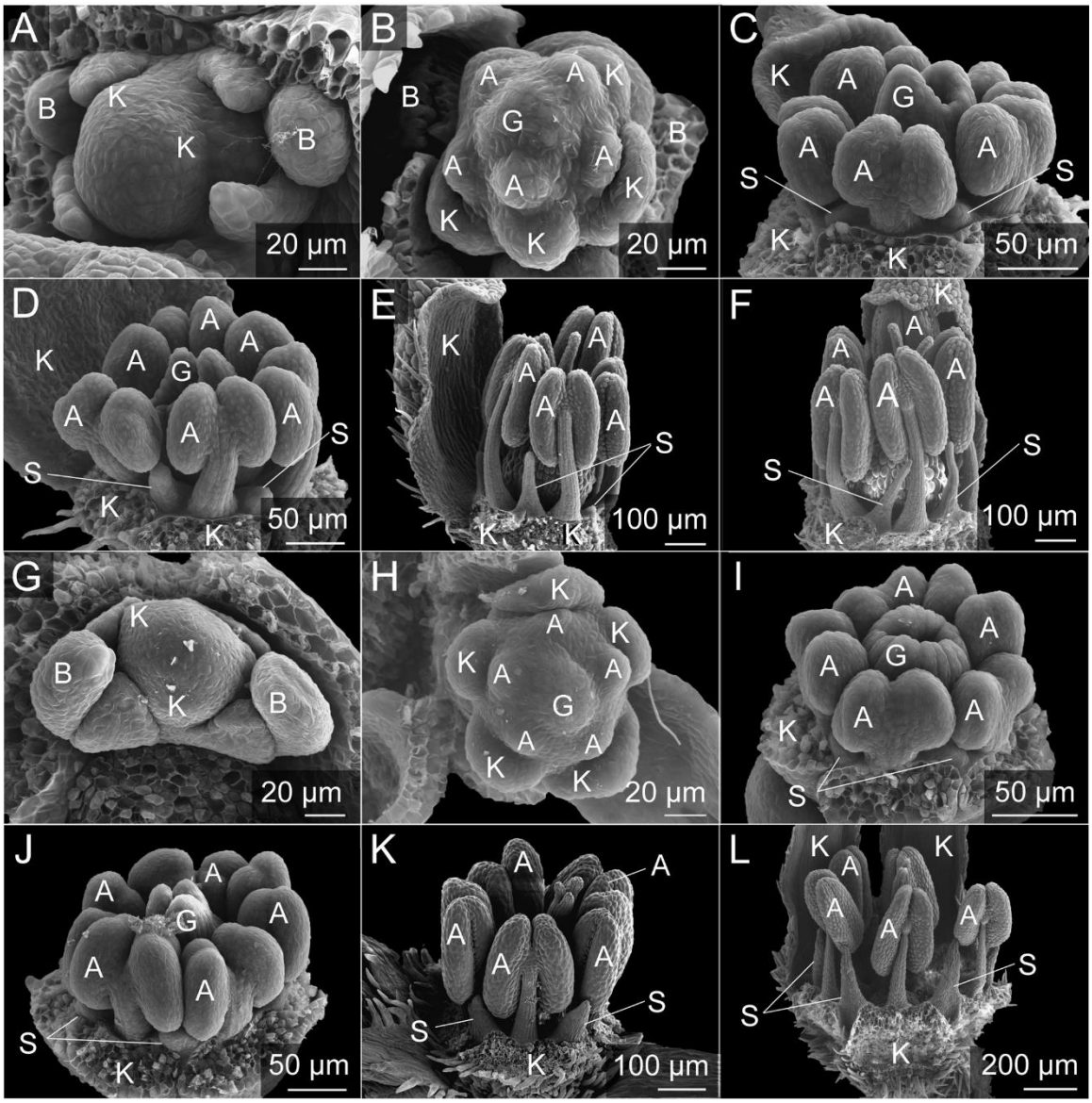

Figure 1. Scanning electron micrographs of *Paronychia* floral development. (A) *P. baldwinii* sepal initiation. (B) *P. baldwinii* anther initiation. (C) *P. baldwinii* initiation of staminodes and filaments and anther enlargement. (D) *P. baldwinii* elongation of staminodes and filaments. (E) *P. baldwinii* base of anthers surpassing the tops of ovaries. (F) *P. baldwinii* mature flower. (G) *P. herniarioides* sepal initiation. (H) *P. herniarioides* anther initiation. (I) *P. herniarioides* initiation of staminodes and filaments and anther enlargement. (J) *P. herniarioides* elongation of staminodes and filaments. (K) *P. herniarioides* base of anthers surpassing the tops of ovaries. (L) *P. herniarioides* mature flower. A = anther, G = gynoecium, K = sepal, and S = staminode.

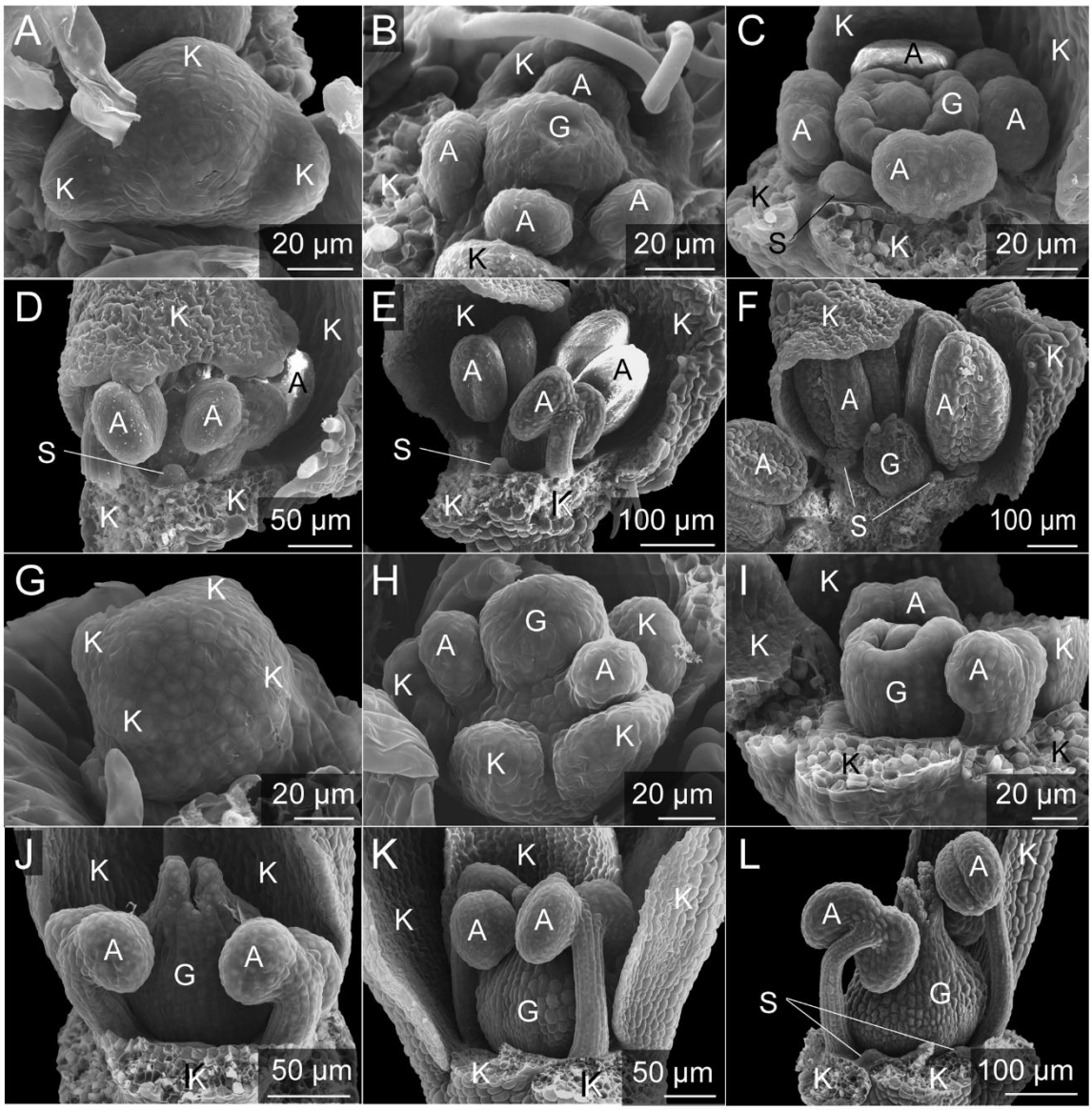

Figure 2. Scanning electron micrographs of *Paronychia* floral development. (A) *P. chartacea* ssp. *chartacea* sepal initiation. (B) *P. chartacea* ssp. *chartacea* anther initiation. (C) *P. chartacea* ssp. *chartacea* initiation of staminodes and filaments and anther enlargement. (D) *P. chartacea* ssp. *chartacea* elongation of staminodes and filaments. (E) *P. chartacea* ssp. *chartacea* base of anthers surpassing the tops of ovaries. (F) *P. chartacea* ssp. *chartacea* mature flower. (G) *P. fastigiata* sepal initiation. (H) *P. fastigiata* anther initiation. (I) *P. fastigiata* initiation of staminodes and filaments and anther enlargement. (J) *P. fastigiata* elongation of staminodes and filaments. (K) *P. fastigiata* base of anthers surpassing the tops of ovaries. (L) *P. fastigiata* mature flower. A = anther, G = gynoecium, K = sepal, and S = staminode.

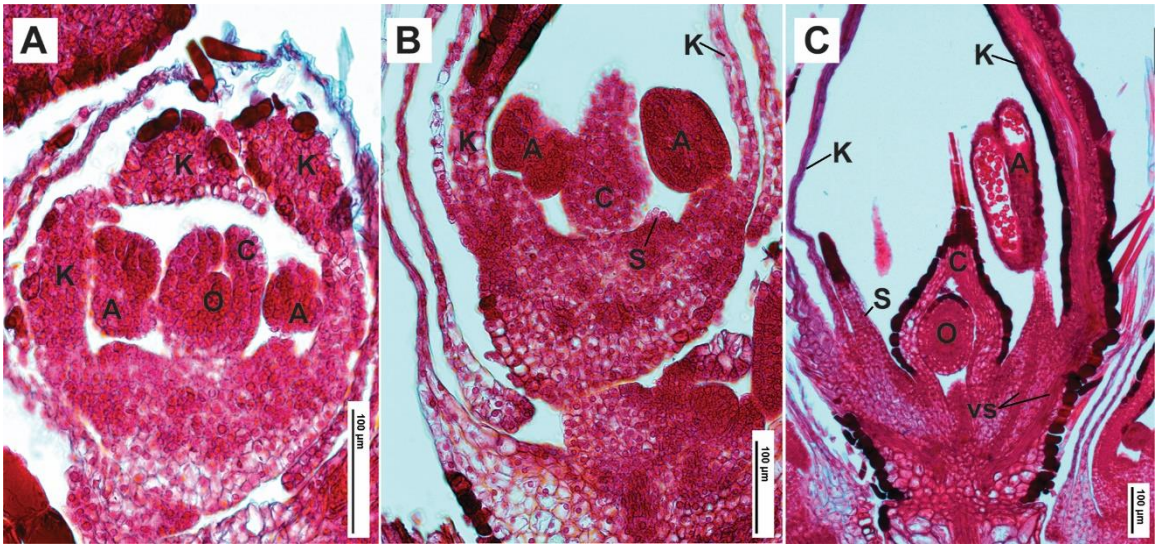

Figure 3. Longitudinal sections of *Paronychia herniarioides*. (A) Flower in early development. (B) Flower mid-development. (C) Mature flower. A = anther, C = carpel, K = sepal, O = ovule, S = staminode, and vs = vascular strand.

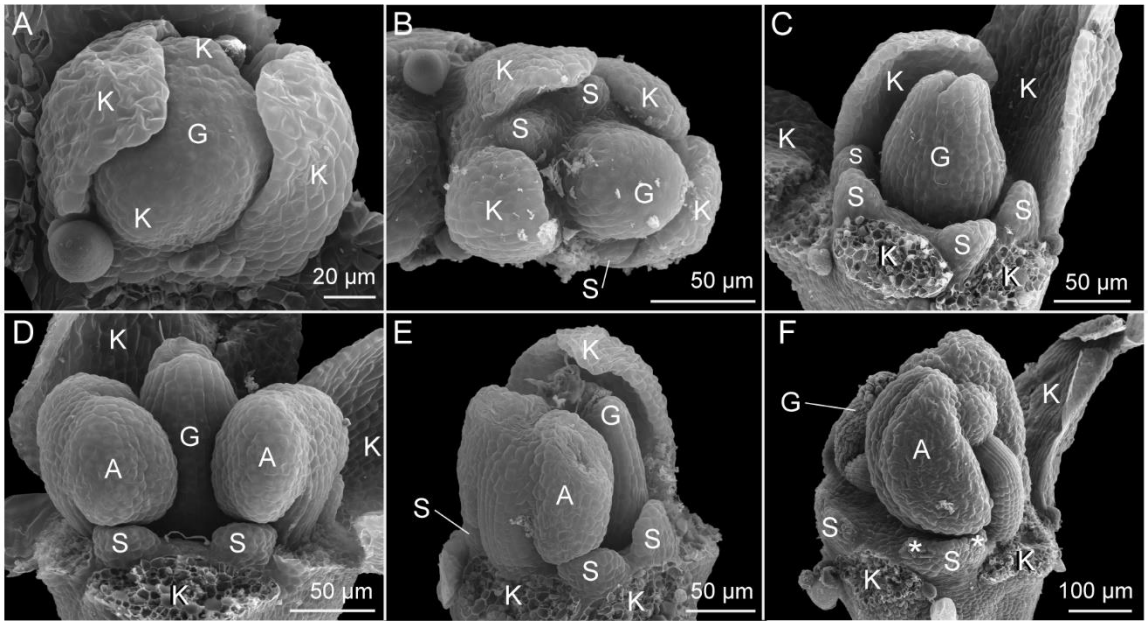

Figure 4. Scanning electron micrographs of *Pollichia campestris* floral development. (A) Early sepal development. (B) Initiation of staminodes. (C) Developing gynoecium and staminodes alternate the sepals. (D) Young stamens opposite the sepals. (E) Developing stamen. (F) Mature flower. A = anther, G = gynoecium, K = sepal, and S = staminode.

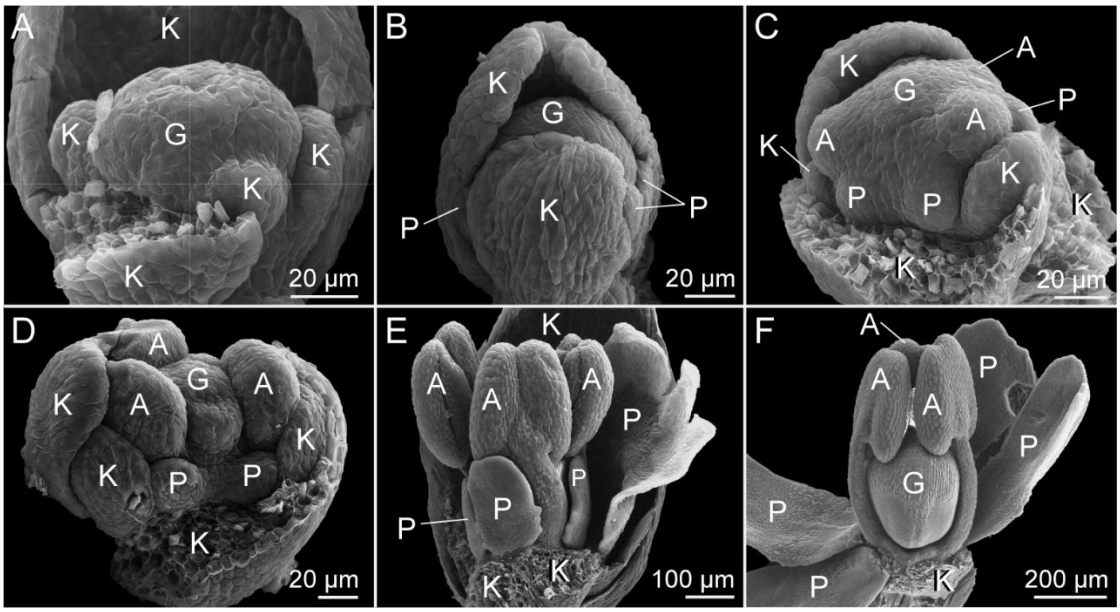

Figure 5. Scanning electron micrographs of *Stipulicida setacea* floral development. (A) Development of the calyx. (B) Initiation of petaloids alternate the sepals. (C) Anther primordia centrifugal to the petaloids. (D) Anthers quickly surpassing the size of petaloids. (E) More developed flower with petaloids laterally expanding. (F) Mature flower. A = anther, G = gynoecium, K = sepal, and P = petaloid.

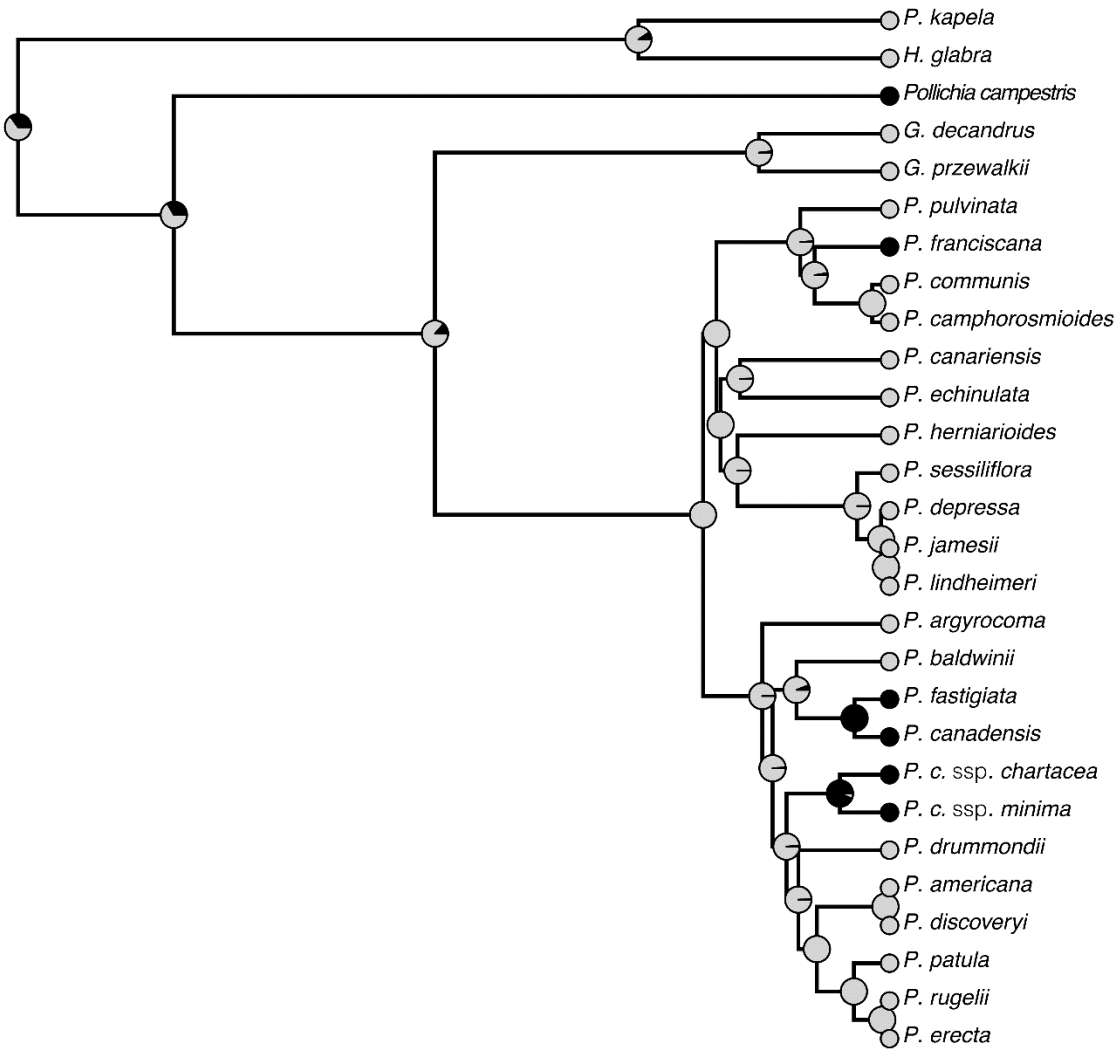

Figure 6. Ancestral state estimates of staminodes (gray = present, black = absent) across the *Paronychia* phylogeny optimized with stochastic character mapping of 1000 simulations. Pie charts at nodes represent the relative posterior probabilities of each state inferred at the node. *Paronychia* is abbreviated as *P.* and *Paronychia chartacea* is abbreviated as *P. c*.

Appendix S1. Staminode matrix, indicating the presence (1) or absence (0) of staminodes in *Paronychia* (Caryophyllaceae) and close relatives.

Species	Staminode
Paronychia erecta	1
Paronychia rugelii	1
Paronychia patula	1
Paronychia discoveryi	1
Paronychia americana	1
Paronychia drummondii	1
Paronychia chartacea ssp. *minima*	0
Paronychia chartacea ssp. *chartacea*	0
Paronychia canadensis	0
Paronychia fastigiata	0
Paronychia baldwinii	1
Paronychia argyrocoma	1
Paronychia lindheimeri	1
Paronychia jamesii	1
Paronychia depressa	1
Paronychia sessiliflora	1
Paronychia herniarioides	1
Paronychia echinulata	1
Paronychia canariensis	1
Paronychia camphorosmioides	1
Paronychia communis	1
Paronychia franciscana	0
Paronychia pulvinata	1
Gymnocarpos przewalskii	1
Gymnocarpos decandrus	1
Pollichia campestris	1
Herniaria glabra	1
Paronychia kapela	1

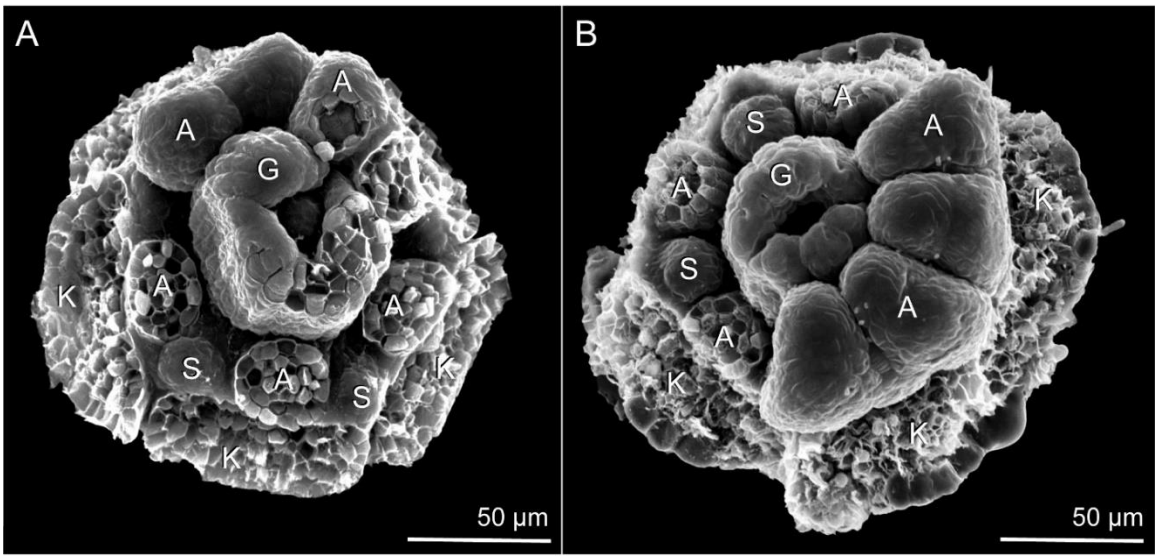

Figure S1. Scanning electron micrographs showing androecial position when staminodes first initiate in *Paronychia*. (A) *P. herniarioides* flower. (B) *P. chartacea* ssp. *chartacea* flower. A = anther, G = gynoecium, K = sepal, and S = staminode.

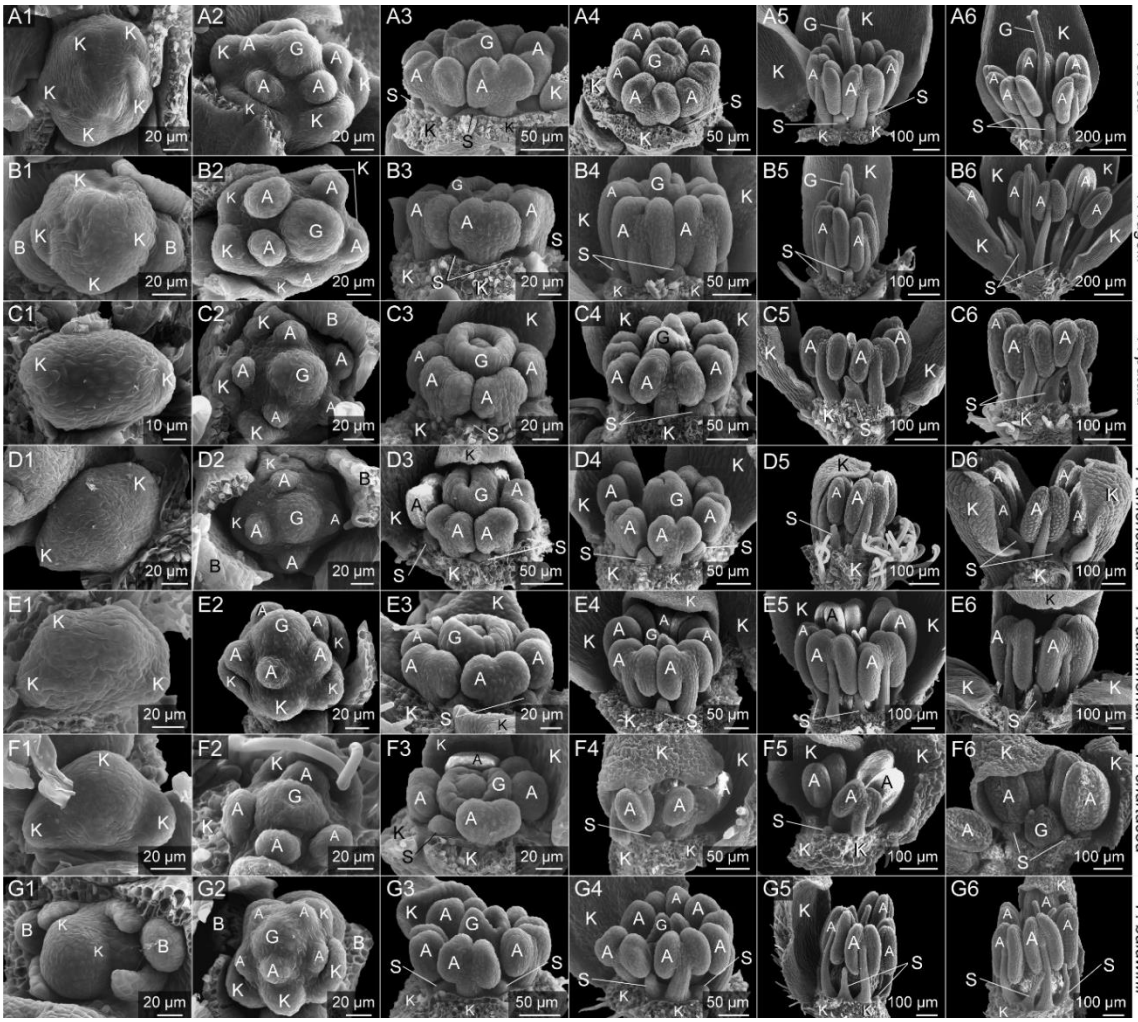

Figure S2. Scanning electron micrographs of *Paronychia* floral development (the first seven of fourteen species from the phylogeny in Figure S1). Each row is comprised of a species, and each column represents a different stage of development. Column 1 is sepal initiation. Column 2 is anther initiation. Column 3 is initiation of staminodes and filaments and anther enlargement. Column 4 is elongation of staminodes and filaments. Column 5 is the base of anthers surpassing the tops of ovaries. Column 6 is mature flowers. A = anther, B = stipular bract, G = gynoecium, K = sepal, and S = staminode.

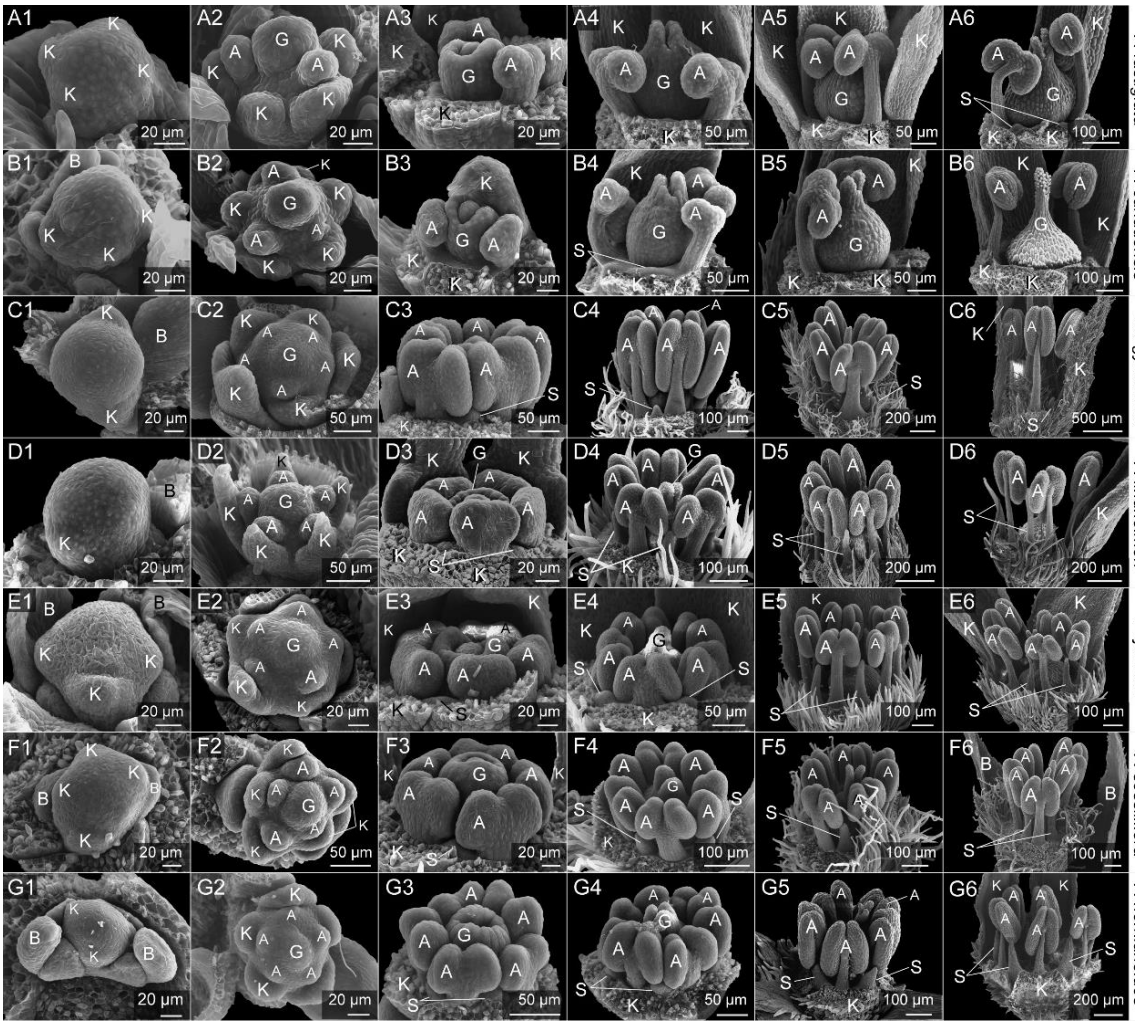

Figure S3. Scanning electron micrographs of *Paronychia* floral development. Each row is comprised of a species, and each column represents a different stage of development. Column 1 is sepal initiation. Column 2 is anther initiation. Column 3 is initiation of staminodes and filaments and anther enlargement. Column 4 is elongation of staminodes and filaments. Column 5 is the base of anthers surpassing the tops of ovaries. Column 6 is mature flowers. A = anther, B = stipular bract, G = gynoecium, K = sepal, and S = staminode.

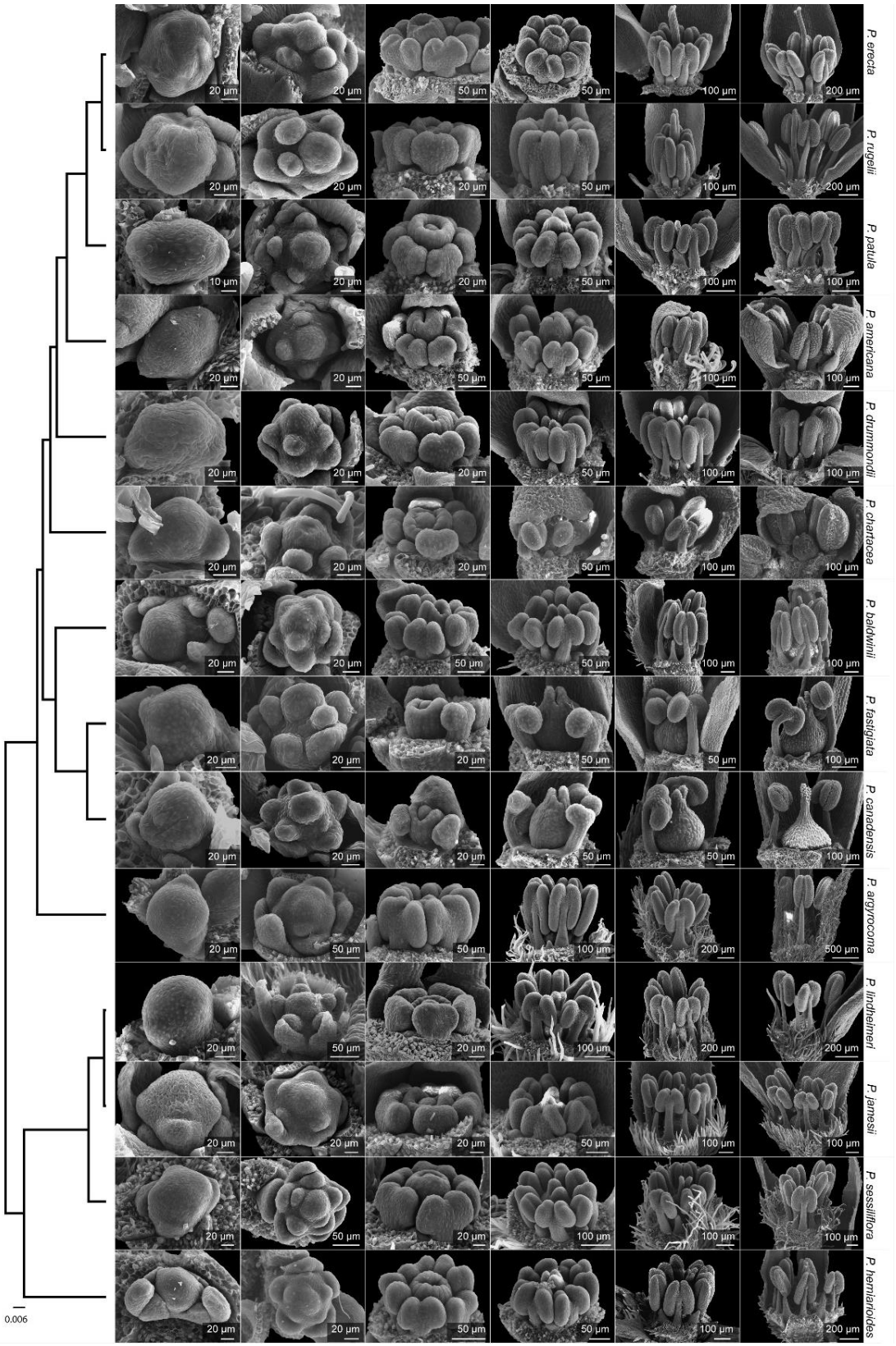

Figure S4. Phylogeny of developmental series of sampled *Paronychia* that combines Figures S1 and S2.

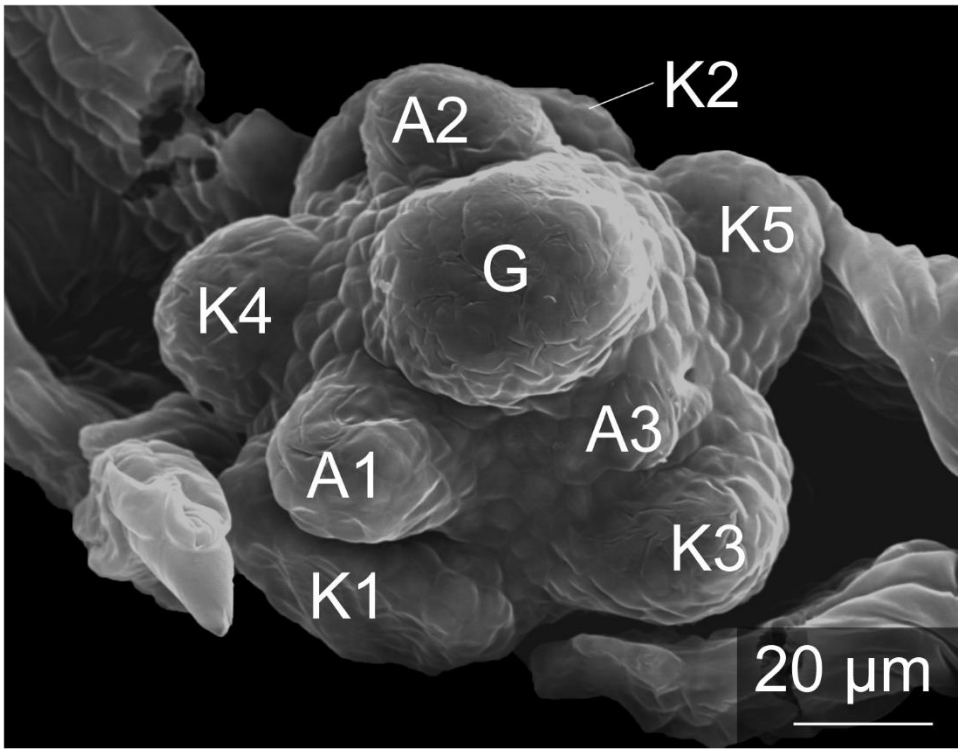

Figure S5. Scanning electron micrograph of a young Paronychia canadensis flower (enlargedfrom Figure S3 B2). The order of developing organs is indicated numerically. A = anther, G =gynoecium, K = sepal.

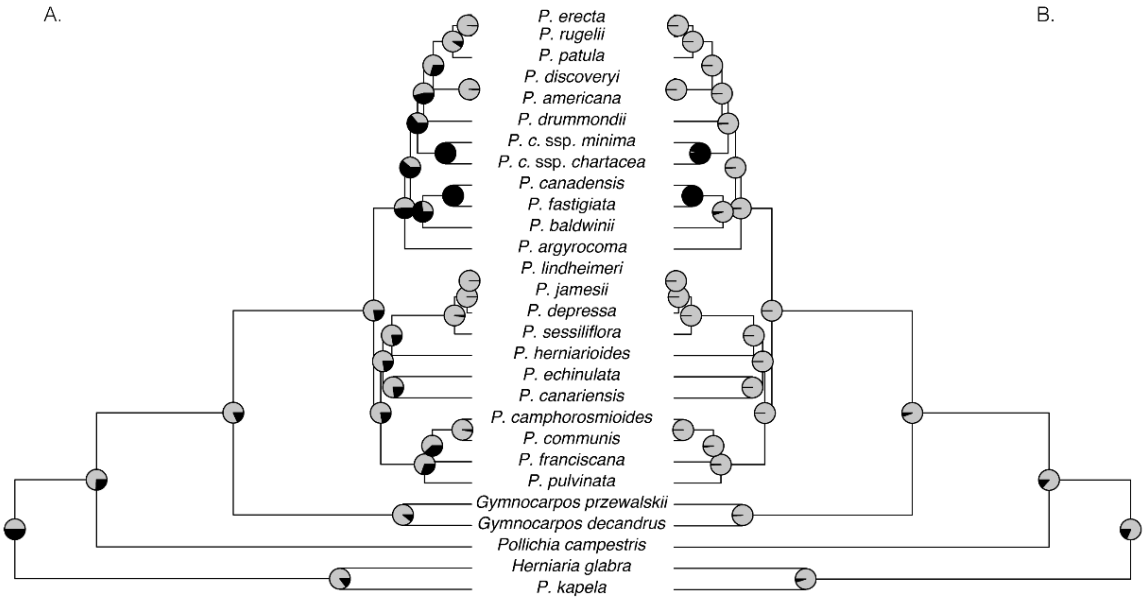

Figure S6. Ancestral character estimations with the (A) all-rates-different and (B) equal-rates model. Pie charts represent proportion of the likelihood estimate for staminodes being present (gray) or absent (black). *Paronychia* is abbreviated as *P*. and *Paronychia chartacea* is abbreviated as *P. c*.